PALEOBIOLOGY
A PUBLICATION OF THE
Paleontological
S O C I E T Y

Morphological innovation and the evolution of hadrosaurid dinosaurs

Thomas L. Stubbs ⓘ, *Michael J. Benton, Armin Elsler* ⓘ, *and Albert Prieto-Márquez*

Abstract.—The hadrosaurids were a successful group of herbivorous dinosaurs. During the Late Cretaceous, 100 to 66 million years ago, hadrosaurids had high diversity, rapid speciation rates, and wide geographic distribution. Most hadrosaurids were large bodied and had similar postcranial skeletons. However, they show important innovations in the skull, including disparate crests that functioned as socio-sexual display structures, and a complex feeding apparatus, with specialized jaws bearing dental batteries. Little is known about the macroevolutionary processes that produced these evolutionary novelties. Here we provide novel perspectives using evolutionary rate and disparity analyses. Our results show that hadrosaurid cranial evolution was complex and dynamic, but their postcranial skeleton and body size were conservative. High cranial disparity was achieved through multiple bursts of phenotypic innovation. We highlight contrasting evolutionary trends within hadrosaurids between the disparate facial skeleton and crests, which both showed multiple high-rate shifts, and the feeding apparatus, which had low variance and high rates on a single phylogenetic branch leading to the diverse Saurolophidae. We reveal that rapid evolutionary rates were important for producing the high disparity of exaggerated crests and present novel evidence that the hadrosaurid diversification was linked to both a key adaptive innovation in the feeding apparatus and multiple bursts of innovation in socio-sexual displays.

Thomas L. Stubbs, Michael J. Benton, and Armin Elsler. School of Earth Sciences, University of Bristol, 24 Tyndall Avenue, Bristol BS8 1TQ, U.K. E-mail: tom.stubbs@bristol.ac.uk, mike.benton@bristol.ac.uk, armin.elsler@ bristol.ac.uk

Albert Prieto-Márquez.* Field Museum of Natural History, 1400 S. Lake Shore Drive, Chicago, Illinois 60605, U.S.A. *Present address: Institut Català de Paleontologia Miquel Crusafont, Universitat Autònoma de Barcelona, Carrer de l'Escola Industrial 23, 08201 Sabadell, Spain. E-mail: albert.prieto@icp.cat

Introduction

Evolutionary diversifications are commonly associated with adaptive radiations, when "key innovations" open new adaptive zones linked to ecological opportunities (Simpson 1953; Schluter 2000; Yoder et al. 2010; Simões et al. 2016). However, not all evolutionary diversifications are directly linked to new ecological adaptations (Rabosky 2017). For example, speciation, high diversity, and morphological variation may be driven by socio-sexual selective factors (Wagner et al. 2012; Rabosky 2017). The fossil record provides insights into evolutionary diversifications across large spatiotemporal scales in geological time (Benton 2015). Methodological advancements and the availability of large phylogenies and morphological data sets allow researchers to test patterns and processes of morphological evolution quantitatively, including evolutionary rate and disparity dynamics in highly

successful groups (e.g., Brusatte et al. 2014; Hopkins and Smith 2015; Close et al. 2015; Benson et al. 2018).

Hadrosauroids were a hugely diverse and abundant clade of herbivorous ornithopod dinosaurs (Horner et al. 2004; Prieto-Márquez 2010a). These megaherbivores were important components in the Late Cretaceous (100–66 million years ago) ecosystems of Eurasia, Antarctica, and the Americas (Prieto-Márquez 2010b). Within hadrosauroids, the clade Hadrosauridae (hadrosaurids) radiated significantly during the latest Cretaceous (Santonian–Maastrichtian) (Fig. 1). Quantitative studies show that hadrosaurids had high taxic diversity (Lloyd et al. 2008; Butler et al. 2009) and notably high speciation rates when compared with other contemporaneous dinosaurian clades (Sakamoto et al. 2016). The postcranial skeleton of hadrosaurids was apparently morphologically conservative, with a consistent
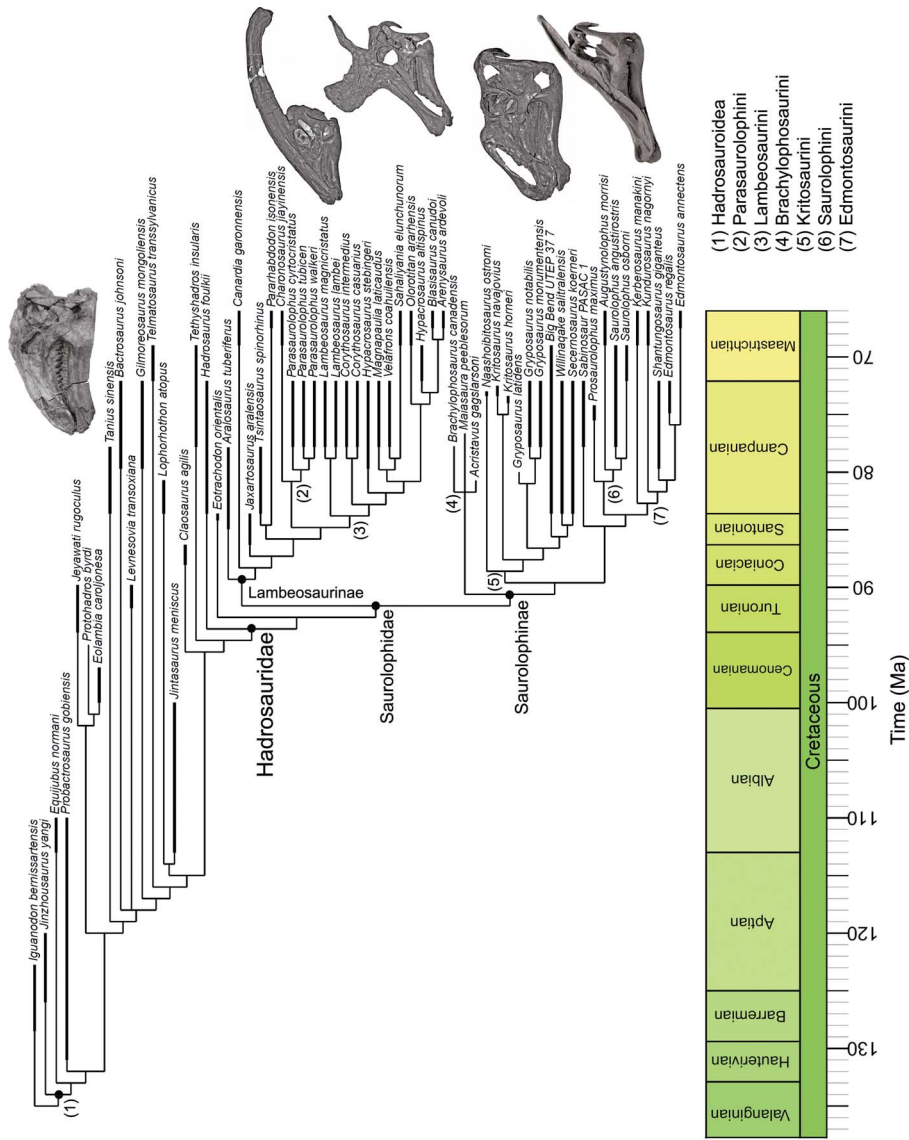
FIGURE 1.   Time-scaled phylogeny of hadrosauroids. The cladogram is a strict consensus tree generated using the four most parsimonious trees from Prieto-Márquez et al. (2016). The thicker lines illustrate the upper and lower bounds of stratigraphic ranges. Major clades are highlighted. The figured skulls are from *Equijubus normani*, *Parasaurolophus walkeri*, *Lambeosaurus lambei*, *Gryposaurus notabilis*, and *Saurolophus angustirostris* (from top to bottom).

body plan, and most species were large-bodied (7–14 m in length) (Horner et al. 2004). However, their cranial and mandibular anatomy shows unique and specialized innovations, potentially linked to their success.

Hadrosaurids are famed for their elaborate solid (most species of the subclade Saurolophinae) and hollow (subclade Lambeosaurinae) cranial crests (Evans 2010; Prieto-Márquez et al. 2015) (Fig. 1). These exaggerated ornamental structures were formed by extensive modifications to the nasal and frontal bones in saurolophines and the premaxilla and nasal bones in lambeosaurines, and they manifested as an impressive array of shapes, including tubes, lobes, fans, and rounded plates. Crests could also be formed by soft tissues (Bell et al. 2014). Hadrosaurid crests functioned primarily as visual displays (Hopson 1975; Bell et al. 2014; Prieto-Márquez et al. 2015), and in lambeosaurines the hypertrophied nasal passages inside the crests may have been used for sound production (Weishampel 1997). The visual and potential auditory signals of hadrosaurid crests were likely important factors in socio-sexual selection, potentially being used for mate competition (Evans 2010; Knell and Sampson 2011; Hone et al. 2011; Bell et al. 2014). Socio-sexual selection can lead to a great variety of specialized adaptations, with important macroevolutionary consequences, including higher speciation rates (Panhuis et al. 2001; Knell et al. 2013). Crests, such as those in hadrosaurids, represent an important innovation and a source of morphological disparity that is disconnected from traditional macroevolutionary "adaptive zones" (Simpson 1953), as they have no role in the acquisition of food resources or escape from predators.

Important adaptive innovations are seen in the hadrosaurid feeding apparatus. They evolved histologically and biomechanically complex grinding structures made from multitoothed dental batteries with complex structures (Erickson et al. 2012). This dentition facilitated crushing and shearing, allowing hadrosaurids to master a broad range of herbivorous diets, while not precluding omnivory (Chin et al. 2017). Complex dentition was associated with specialized jaw mechanisms, potentially giving hadrosaurids the ability to "chew" (Norman and Weishampel 1985; Williams et al.

2009; Cuthbertson et al. 2012). The success of hadrosaurids has been attributed to this unique feeding apparatus, and previous macroevolutionary work on ornithopod dental disparity proposed that, once this complex dental battery emerged rapidly in hadrosaurids, there was limited further innovation (Strickson et al. 2016). Hadrosaurids therefore present an interesting test case for comparing agencies of natural and socio-sexual selection, namely their conservative, but highly successful, feeding apparatus, a classic key innovation, and their highly variable "nonadaptive" cranial crests.

In this study, we present a series of evolutionary rate and disparity analyses that uncover the patterns and processes of morphological evolution during the diversification of hadrosauroids. We address several key questions based on our current understanding of hadrosauroid morphological evolution. First, how do evolutionary rate and disparity dynamics vary between their disparate skulls and seemingly conservative postcranial skeletons? Was hadrosaurid cranial disparity achieved through a single evolutionary burst at one position in the tree, or through multiple bursts of innovation? Did the two major hadrosaurid evolutionary novelties, the disparate cranial crests and the successful feeding apparatus, evolve in the same way—were both associated with a single or multiple evolutionary bursts? Finally, as body-size disparity was a key aspect of dinosaurian evolution and a potential factor in niche partitioning (Barrett 2014; Benson et al. 2018), we test whether rates of hadrosauroid body-size evolution were homogeneous or a potentially important morphological variable. Our results confirm that hadrosauroid skull evolution was dynamic, while their postcranial skeleton was morphologically conservative. Body-size change is ruled out as an important source of innovation. Importantly, we show that the unique hadrosaurid jaw apparatus evolved fast and then stabilized at the root of the clade, whereas the cranial crests kept diversifying in several bursts of rapid evolution throughout hadrosaurid evolution. This highlights contrasting evolutionary dynamics between adaptive and nonadaptive morphological innovations during the diversification of hadrosauroid dinosaurs.

Material and Methods

Hadrosauroid Phylogeny

The hadrosauroid phylogenies used in this study are from Prieto-Márquez et al. (2016). Their study included 60 hadrosauroid species and the out-group *Iguanodon*, and four most parsimonious trees (MPTs) were generated using maximum parsimony analysis. Overall, hadrosauroid interrelationships were well resolved, with uncertainty only in the positions of *Levnesovia* and *Bactrosaurus* and the interrelationships of brachylophosaurin saurolophines (Fig. 1). In this study we perform rate analyses on all four MPTs to gauge the influence of phylogenetic uncertainty. Results are summarized using consensus trees, and individual MPTs are presented in the Supplementary Material.

Phylogenetic Time-scaling

Our evolutionary rate analyses required phylogenies with estimated branch durations. Geological ages for terminal taxa were needed first. Precise temporal occurrence data are rarely known for hadrosauroids, and in most cases, taxon durations represent the bounds of the geological formation(s), stage(s) or substage(s) in which referred fossils are known. Therefore, hadrosauroid ages were recorded as first appearance dates (FADs) and last appearance dates (LADs), using data collected from the primary literature and the geological time scale of Walker et al. (2013) (data in the Supplementary Material S1).

There are multiple methods available for producing time-calibrated phylogenies, and the choice of method can impact results (Bapst 2014; Soul and Friedman 2017). To account for this, we implement two popular time-scaling approaches, the "Hedman" method and the "minimum branch length" (MBL) approach. The Hedman method uses Bayesian statistics to date nodes, incorporating probability distribution constraints derived from successive out-group taxa ages (Hedman 2010). We utilized a whole-tree extension of the Hedman algorithm using the R functions from Lloyd et al. (2016). Successive out-group taxa that predate the hadrosauroid plus *Iguanodon* in-group were required to date the nodes close to, and including, the root. Guided by the supertree from Strickson et al. (2016),

which is a composite topology derived from six phylogenetic studies (Butler et al. 2011; Makovicky et al. 2011; McDonald 2012; Ősi et al. 2012; Norman 2015; Prieto-Márquez et al. 2016), we used the occurrence dates of the following out-group taxa: *Kukufeldia*, *Uteodon*, *Camptosaurus*, *Callovosaurus*, *Agilisaurus*, *Lesothosaurus*, *Pisanosaurus*, *Marasuchus*, and *Euparkeria* (ages are listed in the Supplementary Material S1). The MBL dating method uses the age of the oldest descendant to determine internal node ages. When branches are recovered with durations less than an arbitrarily set threshold, they are substituted with a fixed MBL (here we use 1 Myr) (Laurin 2004). The Hedman dating method is considered to be superior to the MBL approach (Lloyd et al. 2016), so here we use the MBL method only in ancillary analyses to check that our results are consistent.

Dating uncertainty for terminal taxa was incorporated when time-scaling the phylogenies. We randomly selected a point age for each taxon from a uniform distribution between its FAD and LAD (dates reflecting bounds of precise temporal occurrence or range) and performed 100 dating replicates for each MPT. In total, 800 time-scaled hadrosauroid phylogenetic trees were used in the evolutionary rate analyses: 100 replicates for each of the four MPTs, for both the Hedman and MBL dating approaches.

Morphological Data

To test rates of skeletal character evolution, we used the discrete morphological character data set from Prieto-Márquez et al. (2016). In total, 273 morphological characters are included, describing variation from the entire skeleton (see the Supplementary Material S1). The data set has good coverage of the non-hadrosaurid hadrosauroid grade and both major hadrosaurid subclades; the Lambeosaurinae and Saurolophinae. The data set was partitioned to examine evolutionary rates in specific anatomical subregions. The most basic division was to examine rates in the skull, including the cranium, mandible, and teeth (189 characters), versus the postcranial skeleton (84 characters). Additionally, we divided the skull into separate components: the facial skeleton, the crest-

forming elements, and feeding characters. The facial skeleton includes cranial characters, but excludes the braincase, the mandible, and dentition (107 characters). Crest morphology includes characters primarily from the premaxilla and nasal bones and characters relevant to the formation and shape of crests (63 characters). Feeding-related characters are derived from the mandible and dentition (48 characters). Rate analyses were performed separately on these five partitions.

For body-size evolutionary rate analyses, we used maximum femur length as a proxy for hadrosauroid body mass. Femur length is a popular proxy for overall body mass in tetrapods (Carrano 2006), whereas some studies also use stylopodial shaft circumference (e.g., Benson et al. 2018). We selected femur lengths, because more data are available for hadrosauroids (37 out of 60 hadrosauroids in our phylogeny, but the other 23 taxa lacked adequate femora). Femur length data are from Benson et al. (2018), and this data set could not be expanded further through additional museum visits. Data were $\log_{10}$ transformed before rate analyses (see the Supplementary Material S1).

Discrete Character Evolutionary Rates

Rates of character evolution were examined using maximum-likelihood methods. All character rate calculations were performed in R (R Core Team 2018), using the *DiscreteCharacterRate* function from the package 'Claddis' (Lloyd 2016), and ancestral states were calculated using the *rerootingMethod* function in the R package 'phytools' (Revell 2012). We used protocols established by previous studies (e.g., Lloyd et al. 2012; Brusatte et al. 2014; Hopkins and Smith 2015; Wang and Lloyd 2016; Herrera-Flores et al. 2017). The separate analyses required the time-scaled phylogenies and the five partitioned character data sets as input. Rate calculations were based on the number of character changes observed along a branch relative to the duration of that branch. Importantly, the calculations also factored in branch completeness as a denominator (Wang and Lloyd 2016). This is important, because the calculations were based on multiple coded morphological characters (here ranging from 189 to 48 characters), and fossil incompleteness

and character inapplicability will introduce varying degrees of missing data (both for terminal taxa and reconstructed ancestral nodes). This could influence chances of observing character changes. Therefore, per-branch rates were based on changes per character per lineage million years.

Significance tests were used to examine heterogeneous evolutionary rates and to identify branches with notable rate deviations. Rather than focusing on absolute rate values, we followed previous studies and tested whether all individual branches in a tree exhibit higher or lower rates of morphological evolution than the pooled rate for the rest of the tree (Lloyd et al. 2012; Brusatte et al. 2014; Hopkins and Smith 2015; Wang and Lloyd 2016; Herrera-Flores et al. 2017). To determine statistical significance, we used branch likelihood ratio tests, comparing a single rate model (homogeneous rates across the tree) and a two-rate model (individual branch rates different from the rest of the tree). Each branch test gives a *p*-value, and, following published protocols, we use an alpha threshold of 0.01 to assess significance, with Benjamini-Hochberg false discovery rate correction for multiple comparisons (Benjamini and Hochberg 1995; Lloyd et al. 2012; Brusatte et al. 2014; Hopkins and Smith 2015; Wang and Lloyd 2016; Herrera-Flores et al. 2017). In the main text, results from the branch likelihood tests are summarized on a strict consensus tree derived from the four separately analyzed MPTs, incorporating a total of 400 Hedman-dated phylogenies. We use pie charts to illustrate the proportion of dating replicates that showed significantly high or low rates for each branch (Figs. 2, 3).

Body-Size Evolutionary Rates

Body-size evolutionary rates were analyzed in a Bayesian framework using a univariate variable-rates model in BayesTraits v. 2.0.2 and R (Pagel et al. 2004; Venditti et al. 2011; Baker et al. 2016). We examined rate heterogeneity with a Bayesian Markov chain Monte Carlo reversible-jump algorithm. Analyses were run for 10 million (10,000,000) iterations, with parameters sampled every 1000 iterations. The first 10% (1,000,000) of samples were discarded as burn-in, and convergence was assessed based

on effective sample size values >200. This method accounts for phenotypic change along branches assuming a homogeneous Brownian process and also introduces a variable-rates model where branch-specific scalars are incorporated that accommodate branches with greater (or less) phenotypic variance than expected from a homogeneous model (Baker et al. 2016). We assessed the fit of a Brownian (homogeneous) versus variable-rates (heterogeneous) model using Bayes factors (BFs). The marginal likelihood of each model was calculated using stepping-stone sampling, with 100 stones each run for 1000 iterations (Xie et al. 2011). Across hadrosauroid phylogeny, branch-specific rates were reported using the mean scalar parameter. In the main text we present the results using a consensus tree from variable-rates analyses using 400 Hedman-dated phylogenies (four MPTs, each with 100 dating replicates).

Morphological Disparity

Disparity analyses were performed to explore the distribution of skeletal morphological variation in Hadrosauroidea. First, the five partitioned character–taxon morphological data sets were used to calculate a pairwise dissimilarity matrix, based on maximum observable rescaled distances (MORD), using the R package 'Claddis' (Lloyd 2016). From this dissimilarity matrix, disparity was then quantified in four taxonomic bins: the non-hadrosaurid hadrosauroid grade (paraphyletic), Hadrosauridae, Lambeosaurinae, and Saurolophinae. These comparisons were made to test whether the hadrosaurid diversification gave rise to significantly greater morphological disparity than was present in the hadrosauroid grade for each morphological partition and to examine how disparity varied between the two major hadrosaurid subclades. We calculated the variance-based disparity metric within-bin weighted mean pairwise dissimilarity (WMPD). WMPD places greater weighting on pairwise dissimilarities derived from more comparable characters and is robust to sample-size variation (Close et al. 2015). The 95% confidence intervals were generated using a bootstrapping procedure. Supplementary disparity calculations were performed based on unweighted mean pairwise dissimilarity (MPD) and using generalized Euclidean distances.

To further examine morphological diversification in Hadrosauroidea, we generated morphospaces for each anatomical region. The separate MORD matrices were subjected to principal coordinates analysis (PCoA) incorporating Calliez negative eigenvalue correction (Cailliez 1983). Before each PCoA, the function *TrimMorphDistMatrix* from the R package 'Claddis' (Lloyd 2016) was used to iteratively remove selected taxa from the distance matrices that had no shared coded characters (meaning morphological distances were not calculable). Morphospaces were constructed based on PCoA axes 1 and 2, showing the major axes of morphological variation. It is important to note that applying the Cailliez correction notably reduced the proportion of variance expressed by the major PCoA axes when compared with "uncorrected" PCoA (Supplementary Fig. S7). However, in both analyses, the distribution of taxa within morphospace was nearly identical for the major axes, as previously discussed by Hopkins (2016) and Nordén et al. (2018). We used a phylomorphospace approach to visualize the phylogenetic branching pattern. We use a single Hedman-dated phylogeny with the topology of MPT 1 in all phylomorphospace plots. The locations of internal nodes in the phylomorphospaces (the inferred ancestral morphospace positions) were estimated using maximum-likelihood approaches in the R package 'phytools' (Revell 2012).

Results

Rates of Skeletal Character Evolution

Rates of skeletal character evolution were heterogeneous in hadrosauroids. In all 800 trees examined for each of the five morphological partitions, a null test for homogeneous rates across the whole tree was confidently rejected at an alpha threshold of 0.01. This applied to trees time-scaled using both the Hedman and MBL methods. As a result, individual per-branch tests were required to explore the distribution of rate deviations throughout the phylogenies. The frequencies and positions of evolutionary bursts vary for each morphological partition considered, and
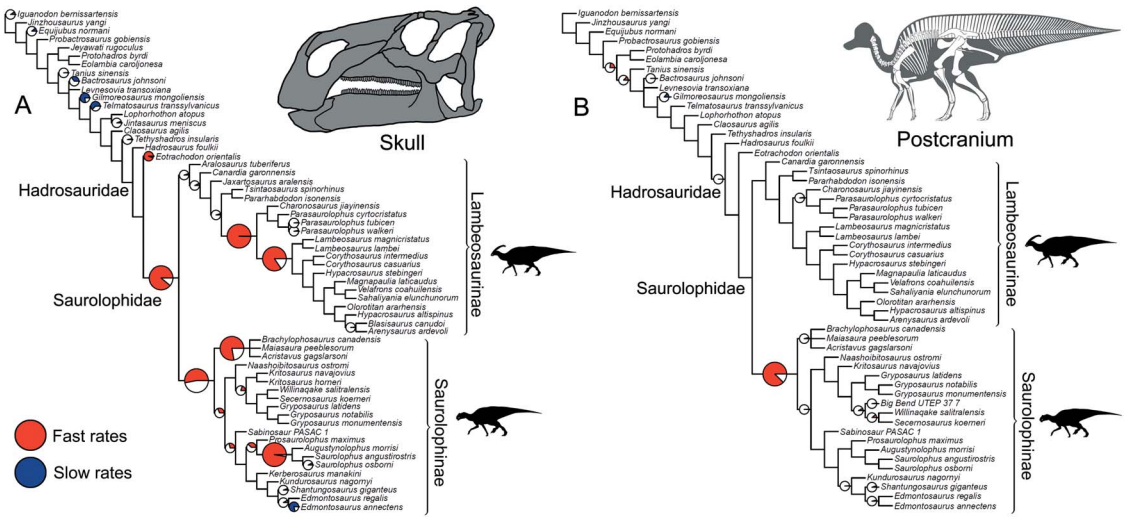
FIGURE 2. Rates of skeletal character evolution in the skull and postcranial skeleton of hadrosauroids. Cladograms illustrate the results from branch likelihood tests for two morphological partitions: skull (cranium and mandible) (A) and postcranial skeleton (B). In both cladograms, results from the branch likelihood tests are summarized on a strict consensus tree derived from four separately analyzed MPTs, each with 100 dating replicates (a total of 400 Hedman-dated phylogenies). Pie charts on branches illustrate the proportion of dating replicates that showed significantly high rates (red), slow rates (blue), or nonsignificant average rates (white). No pie charts are plotted on branches that showed nonsignificant rates in 100% of dating replicates. Branches that showed high rates (red) in more than 50% of dating replicates are doubled in length. See the Supplementary Material for Hedman-based results plotted separately for each MPT (Supplementary Fig. S2) and for results using the MBL dating method (Supplementary Fig. S3). Silhouettes were created by Scott Hartman and were downloaded from http://phylopic.org (Creative Commons license CC BY 3.0).

these are illustrated using consensus trees from the 400 Hedman-dated phylogenies (Figs. 2, 3; MBL results in Supplementary Fig. S3). There is no evidence that the contrasting numbers of significant high- or low-rate branches in the five morphological partitions is a result of variable character-coding completeness (Supplementary Fig. S4). By examining character changes on branches throughout the phylogenies, we confirm that, in all anatomical partitions, significantly high-rate branches reflect large numbers of novel character changes and do not reflect the rapid recycling of already acquired states (Supplementary Fig. S5).

In the skull, likelihood tests show that significantly high evolutionary rates are concentrated in hadrosaurids, while the hadrosauroid grade shows either nonsignificant rates (neither high nor low) or significantly low rates at the tips (e.g., *Gilmoreosaurus* and *Telmatosaurus*) (Fig. 2A). Significantly high rates are seen on the basal hadrosaurid branch giving rise to Saurolophidae. Two branches within Lambeosaurinae also consistently show significantly high rates across dating replicates. Other high-

rate branches are seen at the base of saurolophines and brachylophosaurin saurolophines, and on the branch leading to *Saurolophus* and *Augustynolophus*. These trends are essentially the same when using the MBL dating method (Supplementary Fig. S3). Evolutionary rates in the postcranial skeleton show contrasting results (Fig. 2B): only one branch, at the origin of saurolophines, shows significantly accelerated rates, and no other significant rate shifts are recovered among hadrosaurids. There is very tentative evidence for high postcranial rates more basally in hadrosauroids, but this is not consistently recovered across dating replicates and is recovered in less than 25% of iterations (Fig. 2B).

Subdividing the skull into constituent parts reveals more nuanced trends (Fig. 3). When considering just the facial complex (skull minus the mandible, teeth, and braincase), significantly accelerated rates are recovered at the base of Hadrosauridae and brachylophosaurin saurolophines, and for one branch within more derived lambeosaurines (Fig. 3A). There is some evidence for further facial high-rate
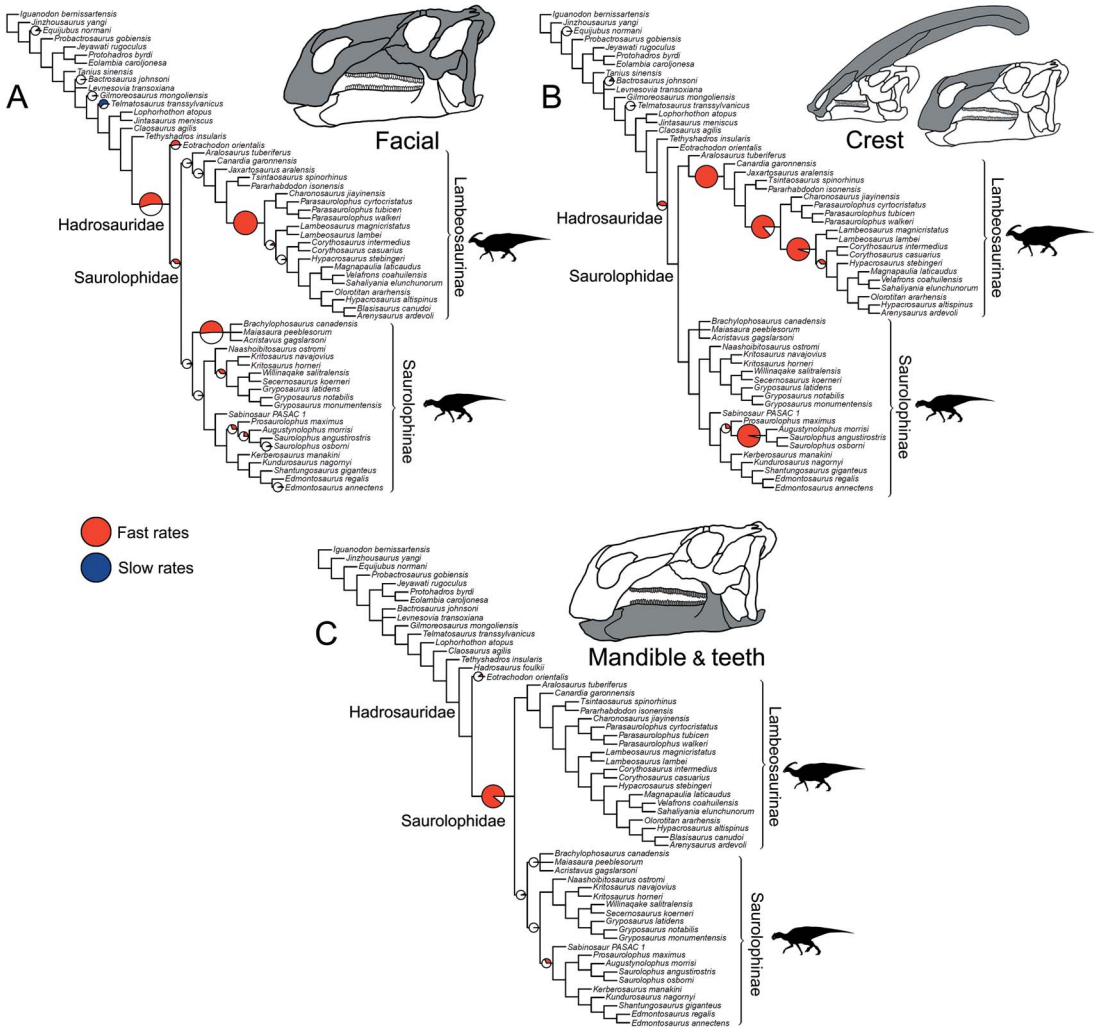
FIGURE 3. Rates of skeletal character evolution in the skulls of hadrosauroids. Cladograms illustrate the results from branch likelihood tests for three morphological partitions: facial bones (A), crest-forming elements (B), and mandible and teeth (C). In all cladograms, results from the branch likelihood tests are summarized on a strict consensus tree derived from four separately analyzed MPTs, each with 100 dating replicates (a total of 400 Hedman-dated phylogenies). Pie charts on branches illustrate the proportion of dating replicates that showed significantly high rates (red), slow rates (blue), or nonsignificant average rates (white). No pie charts are plotted on branches that showed nonsignificant rates in 100% of dating replicates. Branches that showed high rates (red) in more than 50% of dating replicates are doubled in length. See the Supplementary Material for Hedman-based results plotted separately for each MPT (Supplementary Fig. S2) and for results using the MBL dating method (Supplementary Fig. S3). Silhouettes were created by Scott Hartman and were downloaded from http://phylopic.org (Creative Commons license CC BY 3.0).

excursions at the base of Saurolophidae and within Kritosaurini and Saurolophini, but these are not consistently recovered in dating replicates (Fig. 3A). When the phylogenies are dated using the MBL approach, high rates in facial characters are consistently seen at the base of Saurolophidae, but not Hadrosauridae. For the crest-related premaxilla and nasal bones, significantly high rates are seen basally in lambeosaurine hadrosaurids, on the branch leading to all members of the clade except *Aralosaurus* (Fig. 3B). Two further high-rate branches are also consistently recovered in more derived lambeosaurines, at the base of the clade including all members of Parasaurolophini and Lambeosaurini, and again at the
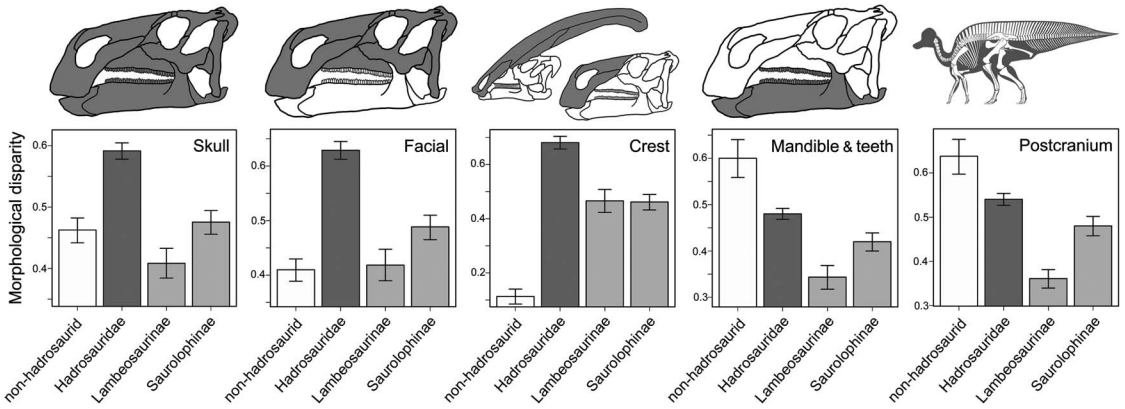
FIGURE 4. Hadrosauroid morphological disparity. Disparity is weighted mean pairwise dissimilarity (WMPD) calculated from maximum observable rescaled distances (MORD). Results are plotted for the entire skull, the facial skeleton, the crest-forming elements, the mandible and teeth, and the postcranial skeleton. Disparity was calculated for four taxonomic bins: the non-hadrosaurid hadrosauroid grade, Hadrosauridae, Lambeosaurinae, and Saurolophinae. Error bars represent 95% confidence intervals generated using a bootstrapping procedure. Disparity results from unweighted MPD and using generalized Euclidean distances are in the Supplementary Material (Supplementary Fig. S6).

branch just for Lambeosaurini. Accelerated rates in crest-related bones are also seen in the Saurolophini within saurolophines (Fig. 3B). There is some support for high crest rates on the basal branch for Hadrosauridae, but this is only recovered in 45% of Hedman-dated trees. Feeding-related characters from the mandible and dentition have significantly accelerated rates on only a single branch, the basal hadrosaurid branch leading to Saurolophidae (Fig. 3C). Nonsignificant rates dominate, and there are no further instances of significant rate shifts in feeding characters within the clade. This result is identical in trees dated using the MBL method (Supplementary Fig. S3).

Hadrosauroid Morphological Disparity

Morphological disparity was unevenly distributed in hadrosauroids (Fig. 4). In the skull, hadrosaurids exhibit significantly greater disparity (WMPD) than the non-hadrosaurid hadrosauroid grade. Within hadrosaurids, saurolophines have greater skull disparity than lambeosaurines. This result is identical when considering only the bones from the facial complex (skull minus the braincase, mandible, and teeth). For the crest-related premaxilla and nasal bones, hadrosaurids once again exhibit significantly greater disparity than the hadrosauroid grade, with the magnitude of difference being even more than when all skull or facial bones are considered. For crest bones, disparity is subequal in lambeosaurines and saurolophines. The hadrosauroid grade has significantly greater disparity in feeding-related characters from the mandible and dentition when compared with hadrosaurids. The same is true when examining the postcranial skeleton (Fig. 4). Disparity results are consistent for unweighted MPD and in calculations using generalized Euclidean distances (Supplementary Fig. S6).

Morphospace trends generally support the conclusions derived from WMPD disparity summary statistics. Morphospaces for the whole skull and just facial bones show that the non-hadrosaurid hadrosauroids occupy a small area of morphospace on both PCoA axes 1 and 2. In contrast, the hadrosaurids have expansive morphospace occupation, and the lambeosaurines and saurolophines radiate on both major axes (Fig. 5A,B). Massive morphospace expansion in hadrosaurids is even more distinct for the crest-related premaxilla and nasal bones (Fig. 5C). Saurolophines are positioned close to the non-hadrosaurid hadrosauroid grade, but they do diverge along PCoA axis 2. The lambeosaurines markedly radiate along PCoA axis 1 and also expand greatly on PCoA axis 2, reflecting the disparate crest morphologies of Parasaurolophini and Lambeosaurini (Fig. 5C). In morphospace for
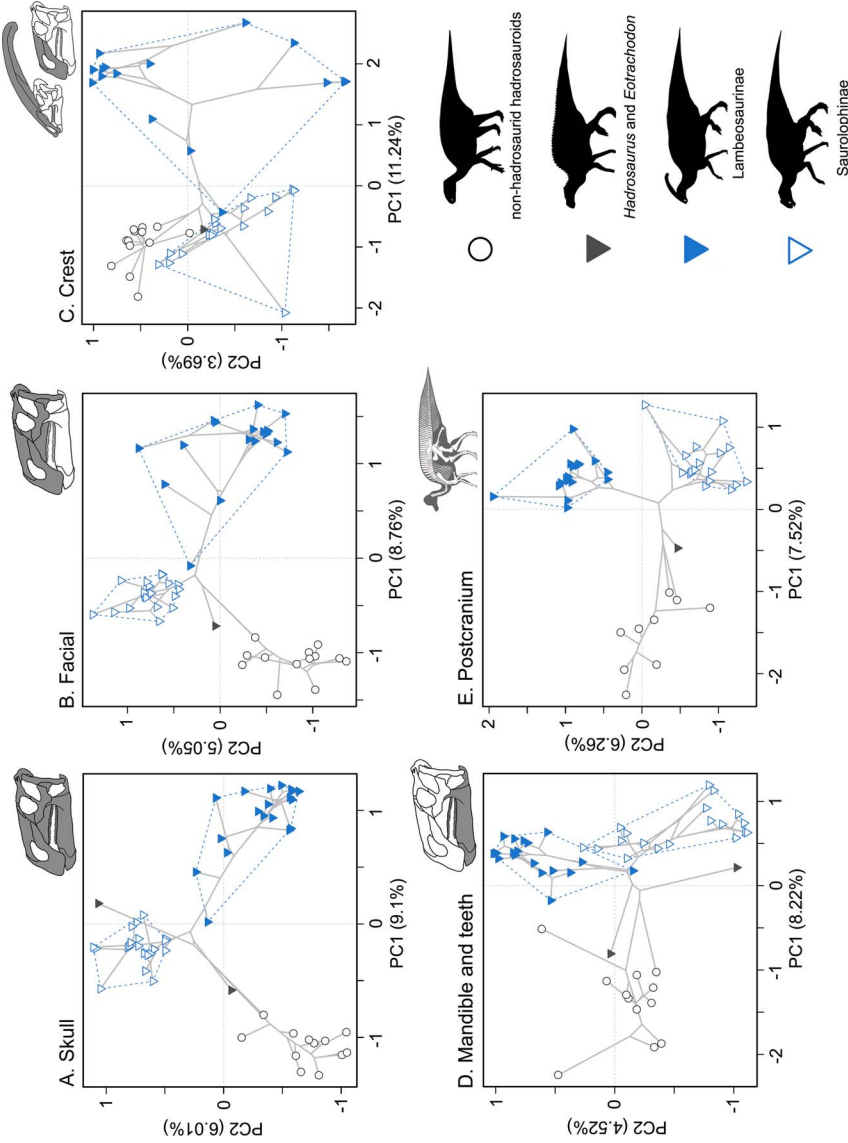
FIGURE 5. Morphospace trends in Hadrosauroidea. Phylomorphospace plots are based on PCoA axes 1 and 2 for five morphological character partitions: skull (55 taxa) (A), facial bones (55 taxa) (B), crest-forming elements (51 taxa) (C), mandible and teeth (52 taxa) (D), and the postcranial skeleton (44 taxa) (E). The major comparative groupings are denoted by different symbols and convex hulls: the non-hadrosaurid hadrosauroid grade (white circles), Hadrosauridae (triangles), Lambeosaurinae (blue filled triangle online) and Saurolophinae (white triangles). The percentage proportional contributions to variance for the plotted axes with/without Calliez correction are: skull (PC 1 9.1%/32.71%, PC 2 6.01%/16.82%) (A), facial bones (PC 1 8.76%/37.63%, PC 2 5.05%/15.5%) (B), crest-forming elements (PC 1 11.24%/50.7%, PC 2 3.69%/10.22% (C), mandible and teeth (PC 1 8.22%/39.05%, PC 2 4.52%/13.8%) (D), and the postcranial skeleton (PC 1 7.52%/28.55%, PC 2 6.26%/18.01%) (E). Plots illustrating the proportional contribution to variance for all PCoA axes for each character partition are presented in the Supplementary Material (Supplementary Fig. S7). Silhouettes were created by Pete Buchholz, Scott Hartman, and Iain Reid and were downloaded from http://phylopic.org (Creative Commons license CC BY 3.0).

feeding-related characters from the jaws and dentition, the non-hadrosaurid hadrosauroids show a more pronounced expansion along PCoA axis 1 compared with other anatomical regions (Fig. 5D). In comparison, hadrosaurids are densely concentrated in a relatively limited expanse of PCoA axis 1. This may explain the reduced WMPD value for hadrosaurids in this character subset (Fig. 4). Saurolophines and lambeosaurines do differ in characters of the jaws and dentition, but this divergence is seen on PCoA axis 2 (Fig. 5D). Similar morphospace trends are seen in the postcranial skeleton, where hadrosaurids do not show such expansive occupation along PCoA axis 1 and are densely concentrated (Fig. 5E).

Rates of Body-Size Evolution

A heterogeneous rate (variable-rates) model for body-size evolution in hadrosauroids received mixed support. Across the 400 analyzed Hedman-dated phylogenies, 37.5% showed very strong evidence for heterogeneity (BFs > 10), 79.25% showed strong evidence (BFs > 5), and 92.75% showed positive evidence (BFs > 2). High-rate branches are rare, and they are concentrated at the terminal branches for *Arenysaurus*, *Shantungosaurus*, and *Tethyshadros* (Fig. 6). High-rate internal branches are seen in the clades containing *Shantungosaurus*, *Edmontosaurus regalis*, and *Edmontosaurus annectens*, and *Hypacrosaurus* and *Arenysaurus* (Fig. 6). Body-size rate trends are consistent in trees dated using the MBL scaling method (Supplementary Fig. S9). The support for heterogeneous rates is comparable (36.25% BFs > 10, 76.75% BFs > 5, 90.75% BFs > 2). High rates are seen at the same terminal branches, and relatively slow evolutionary rates dominate.

Discussion

Morphological Innovation and Hadrosaurid Evolution

We show that hadrosaurid skull disparity was achieved through a series of evolutionary bursts driven by high evolutionary rates, both at the base of Hadrosauridae and at more derived positions within lambeosaurines and saurolophines (Figs. 2, 3). Our results also confirm that hadrosauroid skull evolution was complex and dynamic, but their postcranial skeleton became morphologically conservative. Overall skull disparity was significantly greater in hadrosaurids than the paraphyletic grade of non-hadrosaurid hadrosauroids, but the opposite was seen in the postcranial skeleton (Fig. 4).

The role of morphological innovations during evolutionary diversifications is a key topic in evolutionary biology (Simpson 1953; Briggs et al. 1992; Foote 1997; Benton 2015; Simões et al. 2016; Rabosky 2017; Cooney et al. 2017). Our study suggests the hadrosaurid radiation was linked to both multiple bursts of innovation, which generated variety, and to a key innovation, associated with low disparity. This was revealed by dividing the skull into subunits, which highlighted contrasting evolutionary dynamics between the facial complex and crests and characters associated with the feeding apparatus (Figs. 3, 4, 5). We show that high skull disparity was driven by the facial complex and crest-related characters. Both these subunits have significantly greater disparity in hadrosaurids than in the paraphyletic grade of non-hadrosaurid hadrosauroids, and rate analyses pinpoint multiple phylogenetic branches where evolutionary innovation is accelerated. In contrast, mandibular and dental disparity is significantly reduced in hadrosaurids, when compared with their hadrosauroid out-groups, and branch likelihood tests reveal just one high-rate branch at the base of Saurolophidae, the inclusive clade including all saurolophines and lambeosaurines (Figs. 3, 4, 5). Together, these analyses suggest that a significant burst of phenotypic evolution took place on a single phylogenetic branch, leading to the development of the hadrosaurid feeding apparatus, and was followed by limited subsequent changes or a slower pace of evolution, resulting in low variance.

The Hadrosaurid Feeding Apparatus

Directly linking putative key innovations to successful clades is problematic (Rabosky 2017). However, the trends reported here are consistent with those expected when a key innovation facilitates the invasion of a new adaptive zone, leading to increased diversification. Morphological changes that occurred
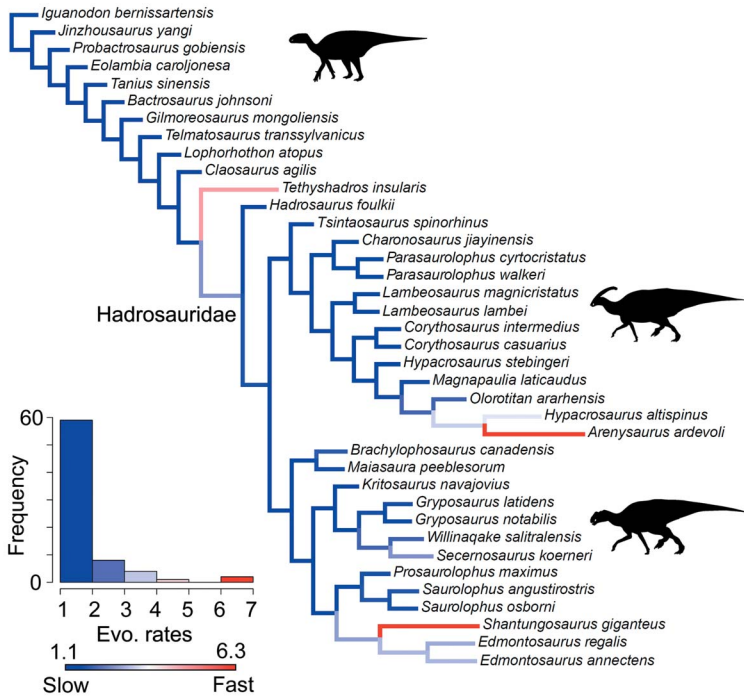
FIGURE 6. Rates of body-size evolution in hadrosauroids estimated using the variable-rates model in BayesTraits. Femur length was used as a proxy for hadrosauroid body mass. The cladogram is a consensus phylogeny showing the results from four separately analyzed MPTs, each with 100 dating replicates (a total of 400 Hedman-dated phylogenies). Phylogenetic branches are colored and scaled by estimates of the mean relative rate of body-size evolution (mean scalar parameter). Branch lengths represent the rate scale parameter, so longer branches equal faster rates. The histogram shows the distribution of mean rates across all edges in the tree. See the Supplementary Material for Hedman-based results plotted separately for each MPT (Supplementary Fig. S8) and for results using the MBL dating method (Supplementary Fig. S9). Silhouettes were created by Scott Hartman and Iain Reid and were downloaded from http://phylopic.org (Creative Commons license CC BY 3.0).

during the evolution of the hadrosaurid dental battery and derived jaw mechanism would have resulted in more sophisticated oral food processing, improving efficiency when processing tough vegetation, decayed wood, and even crustaceans (Erickson et al. 2012; Leblanc et al. 2016; Chin et al. 2017). This advantageous adaptation could have served as a catalyst for diversification. We show that rapid evolutionary rates occur on just one branch at the base of Saurolophidae (Fig. 3C). Saurolophids/ hadrosaurids were incredibly diverse and had high speciation rates in the latest Cretaceous when compared with the grade of non-hadrosaurid hadrosauroids and other ornithopods (Prieto-Márquez 2010a; Strickson et al. 2016; Sakamoto et al. 2016). Unlike Strickson et al. (2016), we did not identify a rate shift at the base of saurolophines, most likely due to

the different taxonomic scope of the studies and the inclusion of mandibular characters in our data.

Our result, that a key innovation is associated with low variance-based disparity in hadrosaurids, is perhaps counterintuitive, but it may suggest that innovation could not substantially diverge from the successful functional ideal, or the trend may result from high hadrosaurid diversity and morphospace saturation (Figs. 4, 5). The morphospace trends documented here show that innovation in hadrosaurid jaws and dentition was expressed on PCoA axis 2, but the group was densely concentrated in a reduced area of morphospace on the primary axis (PCoA axis 1) (Fig. 5D). This apparent saturation pattern mirrors the "morphospace packing" trend reported by Nordén et al. (2018), based on an

analysis of dental and jaw disparity in all Cretaceous herbivorous dinosaurs. When coupled with high diversity, such morphospace saturation or packing can reduce disparity values for distance-based metrics (Fig. 4) (Nordén et al. 2018).

Crest Innovations

An important question in the evolutionary history of dinosaurs, particularly in the hadrosaurids, is how and why the great disparity of exaggerated cranial structures evolved (Hopson 1975; Evans et al. 2009; Evans 2010; Prieto-Márquez and Wagner 2013; Gates et al. 2016; Knapp et al. 2018). Comparative anatomy has revealed the anatomical transformations involved in producing these complex structures. In hadrosaurids, extreme morphological transformations occurred in the premaxilla and nasal bones, involving significant caudal and dorsal migration of facial elements (Evans 2010; Prieto-Márquez and Wagner 2013; Prieto-Márquez et al. 2015). Our study augments this, and places hadrosaurid crest evolution in a phylogenetic comparative context (Fig. 3B). We reveal multiple pulses of rapid phenotypic evolution. One rate shift is seen basally in lambeosaurines, moving them away from the ancestral condition and resulting in morphospace expansion (Fig. 5C). Further high-rate branches are recovered in more derived lambeosaurines, at the base of the clade including all members of the Parasaurolophini and Lambeosaurini, and again on the branch leading to just Lambeosaurini (Fig. 3B). It is interesting that high rates in crest-associated characters are also recovered in the Saurolophini. Members of this clade, *Augustynolophus* and *Saurolophus*, evolved caudally projecting crests on the skull roof, similar in gross morphology to those seen in some lambeosaurines (Fig. 1) (Prieto-Márquez et al. 2015). This implies that rapid evolutionary rates are important for producing these exaggerated structures, a hypothesis that could be explored further in other vertebrate groups.

What was the potential significance of crest innovations in driving hadrosaurid diversity? It is well supported that hadrosaurid crests were display structures and most likely functioned as intraspecific displays (Evans 2010;

Bell et al. 2014; Prieto-Márquez et al. 2015). Other potential functions, such as thermoregulation, respiration, defense, and feeding, have generally been ruled out (Hone et al. 2011). Therefore, these species-specific structures could have been important in driving speciation through socio-sexual selection (Isles 2009). In the ancestral hadrosauroid condition, the crest-forming bones make up the preorbital dorsal surface of the rostrum. In lambeosaurines and convergently in Saurolophini, phenotypic innovations, such as bone lengthening, migration, and rotation, resulted in crests that rise significantly over the skull table. These transformations were associated with fast evolutionary rates (Fig. 3B) and high disparity (Figs. 4, 5), and they highlight a potential common selection pressure for increasing the area, visibility, and elaboration of the displayed structure (Prieto-Márquez et al. 2015). Socio-sexual selection has been widely reported as an important evolutionary driver (Panhuis et al. 2001; Maan and Seehausen 2011; Wagner et al. 2012; Knell et al. 2013). In non-maniraptoriform theropods, the evolution of bony cranial ornamentation has been linked to elevated rates of body-size evolution and gigantism (Gates et al. 2016). Elaborated ornamental plumage has been posited as an important factor in the diversification of Cretaceous birds (Maia et al. 2013; O'Connor et al 2013). In pterosaurs, the development of large display crests represents the major component of cranial and mandibular disparity (Knell et al. 2013; Navarro et al. 2018).

Body Size and Postcranial Evolution

Body-size innovations were not an important factor in the radiation of hadrosauroids. Hadrosauroid body-size evolution was not characterized by bursts of rapid evolutionary change on internal branches. Instead, rate heterogeneity is driven by three exceptional terminal taxa showing higher-rate excursions: *Tethyshadros*, *Arenysaurus*, and *Shantungosaurus* (Fig. 6). *Tethyshadros* and *Arenysaurus* are smaller-bodied species and have been identified as insular dwarfs (Dalla Vecchia 2009; Cruzado-Caballero et al. 2015). *Shantungosaurus* is a gigantic saurolophine (body mass estimated at 17,400 kg), and one of the largest ornithischians

known (Benson et al. 2018). Previous quantitative studies of dinosaurian body-size evolution have documented high-rate shifts more basally in Ornithopoda. This occurred during the Middle to Late Jurassic in iguanodontians, long preceding the radiation of hadrosaurids in the Late Cretaceous (Benson et al. 2014, 2018).

Saurolophines differ from lambeosaurines in displaying accelerated rates of postcranial evolution ancestrally on a single branch (Fig. 2B). This is congruent with anatomical observations that suggest further transformations occurred in certain postcranial regions in saurolophines that did not take place in lambeosaurines. For example, the lambeosaurine ischium is notable for possessing a thumb-shaped process for articulating with the ilium and a "boot-like" process at the end of the ischial shaft (Brett-Surman and Wagner 2007). These features are absent in saurolophines but present in the outgroups. Therefore, the absence of these characters in saurolophines is the derived condition, while lambeosaurines exemplify a retention of these features with little modification.

Future Directions

Hadrosaurid macroevolution shows many interesting parallels to ceratopsians, particularly the derived larger-bodied quadrupedal ceratopsids (Ceratopsidae). Ceratopsids were also important components of Late Cretaceous terrestrial ecosystems, particularly in western North America (Lyson and Longrich 2011). Ceratopsids experienced a rapid radiation in the Late Cretaceous, with fast speciation rates and high taxic diversity (Dodson et al. 2004; Sakamoto et al. 2016). They share ecomorphological characteristics in the jaw (Bell et al. 2009), and ceratopsids evolved a distinctive slicing dentition with complex tissues, aiding the processing of tough plant materials (Erickson et al. 2015). Ceratopsids also possessed conspicuous and highly disparate cranial ornamentation in the form of nasal and postorbital horns and caudodorsally expanded parieto-squamosal frills (Brown and Henderson 2015). These structures likely functioned as displays in socio-sexual signaling (Hone et al. 2011; Brown and Henderson 2015; Knapp et al. 2018), as well as in combat and for the attachment of jaw musculature (Maiorino et al. 2017). As in hadrosaurids, the postcranial skeleton in neoceratopsians is morphologically conservative (Dodson et al. 2004). Future studies incorporating evolutionary rate and disparity analyses for ceratopsians and other archosaurs may uncover similar dynamics to those reported here and provide further insights into the evolution of adaptive and nonadaptive morphological innovations.

Literature Cited

Baker, J., A. Meade, M. Pagel, and C. Venditti. 2016. Positive phenotypic selection inferred from phylogenies. Biological Journal of the Linnean Society 118:95–115.

Bapst, D. W. 2014. Assessing the effect of time-scaling methods on phylogeny-based analyses in the fossil record. Paleobiology 40:331–351.

Barrett, P. M. 2014. Paleobiology of herbivorous dinosaurs. Annual Review of Earth and Planetary Sciences 42:207–230.

Bell, P., F. Fanti, P. Currie, and V. Arbour. 2014. A mummified duck-billed dinosaur with a soft-tissue cock's comb. Current Biology 24:70–75.

Bell, P. R., E. Snively, and L. Shychoski. 2009. A comparison of the jaw mechanics in hadrosaurid and ceratopsid dinosaurs using finite element analysis. Anatomical Record 292:1338–1351.

Benjamini, Y., and Y. Hochberg. 1995. Controlling the false discovery rate: a practical and powerful approach to multiple testing. Journal of the Royal Statistical Society B 57:289–300.

Benson, R. B. J., N. E. Campione, M. T. Carrano, P. D. Mannion, C. Sullivan, P. Upchurch, and D.C. Evans. 2014. Rates of dinosaur body mass evolution indicate 170 million years of sustained ecological innovation on the avian stem lineage. PLoS Biology 12: e1001853. doi: 10.1371/journal.pbio.1001853.

Benson, R. B. J., G. Hunt, M. T. Carrano, and N. Campione. 2018. Cope's rule and the adaptive landscape of dinosaur body size evolution. Palaeontology 61:13–48.

Benton, M. J. 2015. Exploring macroevolution using modern and fossil data. Proceedings of the Royal Society of London B 282:20150569. doi: 10.1098/rspb.2015.0569.

Brett-Surman, M. K., and J. R. Wagner. 2007. Discussion of character analysis of the appendicular anatomy in Campanian and Maastrichtian North American hadrosaurids—variation and

ontogeny. Pp. 135–169 in K. Carpenter, ed. Horns and beaks: ceratopsian and ornithopod dinosaurs. Indiana University Press, Bloomington.

Briggs, D. E. G., R. A. Fortey, and M. A. Wills. 1992. Morphological disparity in the Cambrian. Science 256:1670–1673.

Brown, C., and D. Henderson. 2015. A new horned dinosaur reveals convergent evolution in cranial ornamentation in Ceratopsidae. Current Biology 25:1641–1648.

Brusatte, S. L., G. T. Lloyd, S. C. Wang, and M. A. Norell. 2014. Gradual assembly of avian body plan culminated in rapid rates of evolution across the dinosaur–bird transition. Current Biology 24:2386–2392.

Butler, R. J., P. M. Barrett, P. Kenrick, and M. G. Penn. 2009. Diversity patterns amongst herbivorous dinosaurs and plants during the Cretaceous: implications for hypotheses of dinosaur/angiosperm co-evolution. Journal of Evolutionary Biology 22:446–459.

Butler, R. J., J. Liyong, C. Jun, and P. Godefroit. 2011. The postcranial osteology and phylogenetic position of the small ornithischian dinosaur Changchunsaurus parvus from the Quantou Formation (Cretaceous: Aptian–Cenomanian) of Jilin Province, north-eastern China. Palaeontology 54:667–683.

Cailliez, F. 1983. The analytical solution of the additive constant problem. Psychometrika 48:305–308.

Carrano, M. T. 2006. Body size evolution in the Dinosauria. Pp. 225–268 in M. T. Carrano, T. J. Gaudin, R. W. Blob, and J. R. Wible, eds. Amniote paleobiology: perspectives on the evolution of mammals, birds, and reptiles. University of Chicago Press, Chicago, Ill.

Chin, K., R. M. Feldmann, and J. N. Tashman. 2017. Consumption of crustaceans by megaherbivorous dinosaurs: dietary flexibility and dinosaur life history strategies. Scientific Reports 7:11163. doi: 10.1038/s41598-017-11538-w.

Close, R. A., M. Friedman, G. T. Lloyd, and R. B. J. Benson. 2015. Evidence for a mid-Jurassic adaptive radiation in mammals. Current Biology 25:2137–2142.

Cooney, C. R., J. A. Bright, E. J. R. Capp, A. M. Chira, E. C. Hughes, C. J. A. Moody, L. O. Nouri, Z. K. Varley, and G. H. Thomas. 2017. Mega-evolutionary dynamics of the adaptive radiation of birds. Nature 542:344–347.

Cruzado-Caballero, P., J. Fortuny, S. Llacer, and J. I. Canudo 2015. Paleoneuroanatomy of the European lambeosaurine dinosaur Arenysaurus ardevoli. PeerJ 3:e802. doi: 10.7717/peerj.802.

Cuthbertson, R. S., A. Tirabasso, N. Rybczynski, and R. B. Holmes. 2012. Kinetic limitations of intracranial joints in Brachylophosaurus canadensis and Edmontosaurus regalis (Dinosauria: Hadrosauridae), and their implications for the chewing mechanics of hadrosaurids. Anatomical Record 295:968–979.

Dalla Vecchia, F. M. 2009. Tethyshadros insularis, a new hadrosauroid dinosaur (Ornithischia) from the Upper Cretaceous of Italy. Journal of Vertebrate Paleontology 29:1100–1116.

Dodson, P., C. A. Forster, and S. D. Sampson. 2004 Ceratopsidae. Pp. 494–513 in D. B. Weishampel, P. Dodson, and H. Osmolska, eds. The Dinosauria. University of California Press, Berkeley.

Erickson, G. M., B. A Krick, M. Hamilton, G. R. Bourne, M. A. Norell, E. Lilleodden, and W. G. Sawyer. 2012. Complex dental structure and wear biomechanics in hadrosaurid dinosaurs. Science 338:98–101.

Erickson, G. M., M. A. Sidebottom, D. I. Kay, K. T. Turner, N. Ip, M. A. Norell, W. G. Sawyer, and B. A. Krick. 2015. Wear biomechanics in the slicing dentition of the giant horned dinosaur Triceratops. Science Advances 1:e1500055. doi: 10.1126/sciadv.1500055.

Evans, D. C. 2010. Cranial anatomy and systematics of Hypacrosaurus altispinus, and a comparative analysis of skull growth in lambeosaurine hadrosaurids (Dinosauria: Ornithischia). Zoological Journal of the Linnean Society 159:398–434.

Evans, D. C., R. Ridgely, and L. M. Witmer. 2009. Endocranial anatomy of lambeosaurine hadrosaurids (Dinosauria: Ornithischia): a sensorineural perspective on cranial crest function. Anatomical Record 292:1315–1337.

Foote, M. 1997. The evolution of morphological diversity. Annual Review of Ecology, Evolution, and Systematics 28:129–152.

Gates, T. A., C. Organ, and L. E. Zanno. 2016. Bony cranial ornamentation linked to rapid evolution of gigantic theropod dinosaurs. Nature Communications 7:12931.

Hedman, M. M. 2010. Constraints on clade ages from fossil outgroups. Paleobiology 36:16–31.

Herrera-Flores, J. A., T. L. Stubbs, and M. J. Benton. 2017. Macroevolutionary patterns in Rhynchocephalia: is the tuatara (Sphenodon punctatus) a living fossil? Palaeontology 60:319–328.

Hone, D. W. E., D. Naish, and I. C. Cuthill. 2011. Does mutual sexual selection explain the evolution of head crests in pterosaurs and dinosaurs? Lethaia 45:139–156.

Hopkins, M. J. 2016. Magnitude versus direction of change and the contribution of macroevolutionary trends to morphological disparity. Biological Journal of the Linnean Society 118:116–130.

Hopkins, M. J., and A. B. Smith. 2015. Dynamic evolutionary change in post-Paleozoic echinoids and the importance of scale when interpreting changes in rates of evolution. Proceedings of the National Academy of Sciences USA 112:3758–3763.

Hopson, J. A. 1975. The evolution of cranial display structures in hadrosaurian dinosaurs. Paleobiology 1:21–43.

Horner, J. R., D. B. Weishampel, and C. A. Forster. 2004. Hadrosauridae. Pp. 438–463 in D. B. Weishampel, P. Dodson, and H. Osmolska, eds. The Dinosauria. University of California Press, Berkeley.

Isles, T. E. 2009. The socio-sexual behaviour of extant archosaurs: implications for understanding dinosaur behaviour. Historical Biology 21:139–214.

Knapp, A., R. J. Knell, A. A. Farke, M. A. Loewen, and D. W. E. Hone. 2018. Patterns of divergence in the morphology of ceratopsian dinosaurs: sympatry is not a driver of ornament evolution. Proceedings of the Royal Society of London B 285:20180312. doi: 10.1098/rspb.2018.0312.

Knell, R. J., D. Naish, J. L. Tomkins, and D. W. E. Hone. 2013. Sexual selection in prehistoric animals: detection and implications. Trends in Ecology and Evolution 28:38–47.

Knell, R. J., and S. Sampson. 2011. Bizarre structures in dinosaurs: species recognition or sexual selection? A response to Padian and Horner. Journal of Zoology 283:18–22.

Laurin, M. 2004. The evolution of body size, Cope's rule and the origin of amniotes. Systematic Biology 53:594–622.

Leblanc, A. R. H., R. R. Reisz, D. C. Evans, and A. M. Bailleul. 2016. Ontogeny reveals function and evolution of the hadrosaurid dinosaur dental battery. BMC Evolutionary Biology 16:152.

Lloyd, G. T. 2016. Estimating morphological diversity and tempo with discrete character-taxon matrices: implementation, challenges, progress, and future directions. Biological Journal of the Linnean Society 118:131–151.

Lloyd, G. T., K. E. Davis, D. Pisani, J. E. Tarver, M. Ruta, M. Sakamoto, D. W. E. Hone, R. Jennings, and M. J. Benton. 2008. Dinosaurs and the Cretaceous terrestrial revolution. Proceedings of the Royal Society of London B 275:2483–2490.

Lloyd, G. T., S. C. Wang, and S. L. Brusatte. 2012. Identifying heterogeneity in rates of morphological evolution: discrete character change in the evolution of lungfish (Sarcopterygii; Dipnoi). Evolution 66:330–348.

Lloyd, G. T., D. W. Bapst, M. Friedman, and K. E. Davis. 2016. Probabilistic divergence time estimation without branch lengths: dating the origins of dinosaurs, avian flight and crown birds. Biology Letters 12:20160609. doi: 10.1098/rsbl.2016.0609.

Lyson, T. R., and N. R. Longrich. 2011. Spatial niche partitioning in dinosaurs from the latest Cretaceous (Maastrichtian) of North America. Proceedings of the Royal Society of London B 278:1158–1164.

Maan, M. E., and O. Seehausen. 2011. Ecology, sexual selection and speciation. Ecology Letters 14:591–602.

Makovicky, P. J., B. M. Kilbourne, R. W. Sadleir, and M. A. Norell. 2011. A new basal ornithopod (Dinosauria, Ornithischia) from the Late Cretaceous of Mongolia. Journal of Vertebrate Paleontology 31:626–640.

Maia, R., D. R. Rubenstein, and M. D. Shawkey. 2013. Key ornamental innovations facilitate diversification in an avian radiation. Proceedings of the National Academy of Sciences USA 110:10687–10692.

Maiorino, L., A. A. Farke, T. Kotsakis, and P. Piras. 2017. Macroevolutionary patterns in cranial and lower jaw shape of ceratopsian dinosaurs (Dinosauria, Ornithischia): phylogeny, morphological integration, and evolutionary rates. Evolutionary Ecology Research 18:123–167.

McDonald, A. T. 2012. Phylogeny of basal iguanodonts (Dinosauria: Ornithischia): an update. PLoS ONE 7:e36745. doi: 10.1371/journal.pone.0036745.

Navarro, C. A., E. Martin-Silverstone, and T. L. Stubbs. 2018. Morphometric assessment of pterosaur jaw disparity. Royal Society Open Science 5:172130. doi: 10.1098/rsos.172130.

Nordén, K. K., T. L. Stubbs, A. Prieto-Márquez, and M. J. Benton. 2018. Multifaceted disparity approach reveals dinosaur herbivory flourished before the end-Cretaceous mass extinction. Paleobiology 44:1–18.

Norman, D. B. 2015. On the history, osteology, and systematic position of the Wealden (Hastings Group) dinosaur *Hypselospinus fittoni* (Iguanodontia: Styracosterna). Zoological Journal of the Linnean Society 173:92–189.

Norman, D. B., and D. B. Weishampel. 1985. Ornithopod feeding mechanisms: their bearing on the evolution of herbivory. American Naturalist 126:151–164.

O'Connor, J., X. Wang, C. Sullivan, X. Zheng, P. Tubaro, X. Zhang, and Z. Zhou. 2013. Unique caudal plumage of *Jeholornis* and complex tail evolution in early birds. Proceedings of the National Academy of Sciences USA 110:17404–17408.

Ősi, A., E. Prondvai, R. J. Butler, and D. B. Weishampel. 2012. Phylogeny, histology and inferred body size evolution in a new rhabdodontid dinosaur from the Late Cretaceous of Hungary. PLoS ONE 7:e44318. doi: 10.1371/journal.pone.0044318.

Pagel, M., A Meade, and D. Barker. 2004. Bayesian estimation of ancestral character states on phylogenies. Systematic Biology 53:673–684.

Panhuis, T. M., R. Butlin, M. Zuk, and T. Tregenza. 2001. Sexual selection and speciation. Trends in Ecology and Evolution 16:364–371.

Prieto-Márquez, A. 2010a. Global phylogeny of Hadrosauridae (Dinosauria: Ornithopoda) using parsimony and Bayesian methods. Zoological Journal of the Linnean Society 159:435–502.

Prieto-Márquez, A. 2010b. Global historical biogeography of hadrosaurid dinosaurs. Zoological Journal of the Linnean Society 159:503–525.

Prieto-Márquez, A., and J. R. Wagner. 2013. The "unicorn" dinosaur that wasn't: a new reconstruction of the crest of *Tsintaosaurus* and the early evolution of the lambeosaurine crest and rostrum. PLoS ONE 8:e82268. doi: 10.1371/journal.pone.0082268.

Prieto-Márquez, A., J. R. Wagner, P. R. Bell, and L. M. Chiappe. 2015. The late-surviving "duck-billed" dinosaur *Augustynolophus* from the upper Maastrichtian of western North America and crest evolution in Saurolophini. Geological Magazine 152:225–241.

Prieto-Márquez, A., G. M. Erickson, and J. A. Ebersole. 2016. A primitive hadrosaurid from southeastern North America and the origin and early evolution of "duck-billed" dinosaurs. Journal of Vertebrate Paleontology 36:e1054495. doi: 10.1080/02724634.2015.1054495.

Rabosky, D. L. 2017. Phylogenetic tests for evolutionary innovation: the problematic link between key innovations and exceptional diversification. Philosophical Transactions of the Royal Society of London B 372:20160417. doi: 10.1098/rstb.2016.0417.

R Core Team. 2018. R: a language and environment for statistical computing. R Foundation for Statistical Computing, Vienna, Austria. http://www.r-project.org, accessed 20 December 2018.

Revell, L. J. 2012. phytools: an R package for phylogenetic comparative biology (and other things). Methods in Ecology and Evolution 3:217–223.

Sakamoto, M., M. J. Benton, and C. Venditti. 2016. Dinosaurs in decline tens of millions of years before their final extinction. Proceedings of the National Academy of Sciences USA 113:5036–5040.

Schluter, D. 2000. The ecology of adaptive radiation. Oxford University Press, Oxford.

Simões, M., L. Breitkreuz, M. Alvarado, S. Baca, J. C. Cooper, L. Heins, K. Herzog, and B. S. Lieberman. 2016. The evolving theory of evolutionary radiations. Trends in Ecology and Evolution 31:27–34.

Simpson, G. G. 1953. The major features of evolution. Columbia University Press, New York.

Soul, L. C., and M. Friedman. 2017. Bias in phylogenetic measurements of extinction and a case study of end-Permian tetrapods. Palaeontology 60:169–185.

Strickson, E., A. Prieto-Márquez, M. J. Benton, and T. L. Stubbs. 2016. Dynamics of dental evolution in ornithopod dinosaurs. Scientific Reports 6:28904. doi: 10.1038/srep28904.

Venditti, C., A. Meade, and M. Pagel. 2011. Multiple routes to mammalian diversity. Nature 479:393–396.

Wagner, C. E., L. J. Harmon, and O. Seehausen. 2012. Ecological opportunity and sexual selection together predict adaptive radiation. Nature 487:366–369.

Walker, J. D., J. W. Geissman, S. A. Bowring, and L. E. Babcock. 2013. The Geological Society of America geologic time scale. GSA Bulletin 125:259–272.

Wang, M., and G. T. Lloyd. 2016. Rates of morphological evolution are heterogeneous in Early Cretaceous birds. Proceedings of the Royal Society of London B 283:20160214. doi: 10.1098/rspb.2016.0214.

Weishampel, D. B. 1997. Dinosaurian cacophony. Bioscience 47:150–159.

Williams, V. S., P. M. Barrett, and M. A. Purnell. 2009. Quantitative analysis of dental microwear in hadrosaurid dinosaurs, and the implications for hypotheses of jaw mechanics and feeding. Proceedings of the National Academy of Sciences USA 106:11194–11199.

Xie, W., P. O. Lewis, Y. Fan, L. Kuo, and M-H. Chen. 2011. Improving marginal likelihood estimation for Bayesian phylogenetic model selection. Systematic Biology 60:150–160.

Yoder, J. B., E. Clancey, S. D. Roches, J. M. Eastman, L. Gentry, W. Godsoe, T. J. Hagey, D. Jochimsen, B. P. Oswald, J. Robertson, *et al.* 2010. Ecological opportunity and the origin of adaptive radiations. Journal of Evolutionary Biology 23:1581–1596.